Matching Layer for Path Loss Reduction in Ultra Wideband Implant Communications

Raúl Chávez-Santiago, Ali Khaleghi, and Ilangko Balasingham, *IEEE Senior Member*

Abstract— **Real-time monitoring of various physiological signals is of utmost importance for the treatment of chronic conditions. Radio technology can enable real-time sensing and collection of physiological data to facilitate timely medication and early pre-hospital management of patients. This can be realized with the aid of implantable biomedical sensors with the capability to transmit wirelessly the collected information to an external unit for display and analysis. Currently, commercial wireless medical implantable sensors operate in frequencies below 1 GHz with narrowband signals. Recently, it has been demonstrated that ultra wideband (UWB) signals could be also used for the radio interface of these devices. However, establishing an implant communication link in the allocated UWB spectrum of 3.1-10.6 GHz is challenging. The attenuation of UWB signals propagating through biological tissues at these frequencies is high. Part of these path losses are caused by the impedance mismatch between the two propagation environments (i.e., air and biological tissues) that constitute an implant communication link. This mismatch results in inefficient power transmission of the radio waves. In this paper we propose the use of a layer of dielectric material that can be applied on the patient's skin. The permittivity value of this matching layer has to be chosen such that wave coupling is maximized. Through numerical simulations we determined the appropriate permittivity value of a matching layer for UWB implant communication links in the human thorax for 1–6 GHz. Path loss reduction of up to 10 dB can be obtained in this frequency band. These results can help improve the use of UWB signals for other in-body biomedical devices like the wireless capsule endoscope (WCE).**

I. Introduction

Real-time monitoring of various physiological signals is of utmost importance for the treatment of chronic conditions like diabetes and cardiovascular diseases. Radio technology can enable real-time sensing and collection of physiological data to facilitate timely medication and early pre-hospital management of patients. This can be realized with the aid of implantable biomedical sensors with the capability to transmit wirelessly the collected information to an external unit for display and analysis. Currently, commercial implantable medical sensors operate with narrowband channels in frequencies below 1 GHz, e.g., the medical implant communication services (MICS) band of 401-405 MHz [1]. Although this band offers good propagation behavior through biological tissues allowing the fabrication of reasonably-sized antennas, its limited bandwidth constrains the communication link to low data rates. Recently, it has been suggested that ultra wideband (UWB) signals could be used for the radio interface of in-body sensors and actuators, including the wireless capsule endoscope (WCE) [2]. The WCE has established itself as a very useful diagnostic tool for diseases in the gastrointestinal (GI) tract and would benefit significantly from the use of UWB technology for the communication interface [3].

However, establishing an implant communication link in the allocated UWB spectrum of 3.1-10.6 GHz is challenging. Attenuation of UWB signals propagating through biological tissues at these frequencies is high. Part of these path losses are caused by the impedance mismatch between the two propagation environments (i.e., air and biological tissues) that constitute an implant communication link. This mismatch results in inefficient power transmission of the radio waves. Drawing inspiration from ultrasonic transducers for medical imaging [4], the idea of using a layer of dielectric material that can be applied on the patient's skin to counter the impedance mismatch of UWB implant communication links in 100-1000 MHz was presented in [5]. The permittivity value of this *matching layer* has to be chosen such that the wave coupling is maximized. In this paper we determine the appropriate permittivity value of a matching layer for UWB implant communication links in the human thorax for 1–6 GHz, which covers the part of the UWB spectrum suggested for WCE communication, i.e., 3.1-4.8 GHz [6]. Through numerical simulations we found that the path loss can be reduced up to 10 dB in this frequency band. Besides implant communication in the thorax, this work can be extended to implant communication in the abdomen. We sketch the application of a matching layer for the improvement of UWB WCE systems.

The remainder of the paper is organized as follows: Section II describes the scenario in which the wave propagation was simulated. Section III presents the path loss results for different permittivity values. Section IV discusses the selection of the most appropriate permittivity value for the matching layer. Section V summarizes our conclusions.

Research supported by the Research Council of Norway through the MELODY Project-Phase II (Contract no. 225885). Additional funding was provided by the Health Region Authority/Helse Sør-Øst through the Innovation Grant no. 11/01137-156.

R. Chávez-Santiago is with The Intervention Centre, Oslo University Hospital, NO-0027 Oslo, Norway (+47-230-70010; fax: +47-230-70110; e-mail: raul.chavez-santiago@rr-research.no). He is also with the Institute of Clinical Medicine, University of Oslo, Norway, and the Norwegian University of Science and Technology (NTNU), Trondheim, Norway.

A. Khaleghi is with The Intervention Centre, Oslo University Hospital, and K. N. Toosi University of Technology (e-mail: ali.khaleghi@rr-research.no).

I. Balasingham is with The Intervention Centre, Oslo University Hospital, the Institute of Clinical Medicine, University of Oslo, and NTNU (e-mail: ilangko.balasingham@medisin.uio.no).

978-1-4244-7929-0/14/$26.00 ©2014 IEEE

II. Simulation Scenario

The numerical simulations for this study used the heterogeneous anatomical model depicted in Fig. 1. This model is based on data from the Visual Human Project® of the National Laboratory of Medicine (NLM) [7], in which the human body is represented by voxels with a spatial resolution of 1 mm. This resolution allows the accurate representation of the shape of most of the internal organs. The voxels of the anatomical model were classified according to their different material dielectric properties, i.e., conductivity and permittivity. Thirty-two different types of biological tissues were defined. In order to reduce the simulation time and memory consumption, only the human torso was considered instead of the whole body.

The model of the torso was exposed to an incoming plane wave from the front direction. Electric and magnetic field probes were arranged in a rectangular cube of 140 mm (*w*-axis), 160 mm (*u*-axis), and 80 mm (*v*-axis) inside the thorax as shown in Fig. 1. The probes were separated from each other a distance of 20 mm, 10 mm, and 20 mm in each axis, respectively. The total number of probes was 680 with 85 probes on each plane parallel to the skin (*uv*-plane). Because of the curvature of the torso the probes on the same plane had different distances to the skin. The average depth from the skin to the first plane of probes was 20 mm. The probes were frequency-independent isotropic radiating antennas with a defined polarization and were embedded in different biological tissues. It was assumed that the probe arrays did not have any mutual coupling. The electric-field probes were co-polarized with the incoming wave, i.e., in the propagation direction into the body, whereas the magnetic-field probes were orthogonally-polarized to the electric probes. The perfect matching layer (PML) boundary condition was applied, thus the wave reflections from the environment were ignored. The numerical simulations were done on the CST Microwave Studio® platform, which applies the Finite Integration Technique (FIT) to solve the integral form of the Maxwell's equations in the time-domain. The frequency-dependent dielectric properties of the human tissues, i.e., permittivity and conductivity, were taken from [8]. However, in order to reduce the computation time, a simplified equation to describe the frequency-dependent complex permittivity of the human tissues was applied [9].

In order to simulate the matching layer, the entire environment surrounding the torso was filled with a lossless dielectric material, i.e., the matching layer was assumed to be of infinite size. The permittivity of the air was considered to be equal to 1, which is the case of the propagation path without a matching layer. Other different permittivity values that we used were ε_r = 3, 5, 10, 20, 30, 40, 50, 60, and 70, for each of the different dielectric matching layer cases. The incoming plane wave was excited with a UWB Gaussian pulse with –20 dB spectral bandwidth with respect to the peak spectrum value covering 1–6 GHz, respectively, as depicted in Fig. 2. The total energy of the incoming wave for all the simulations was normalized to unity, i.e., the UWB signal energy had a constant value of 0 dB J/m^2 on the body surface.

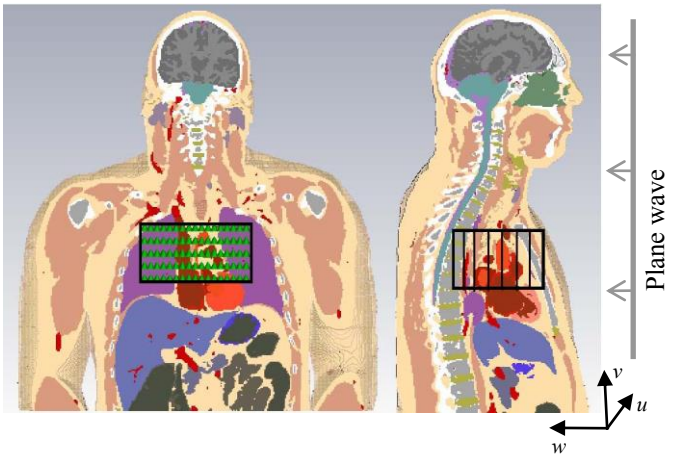

Figure 1. Simulation scenario of the human torso.

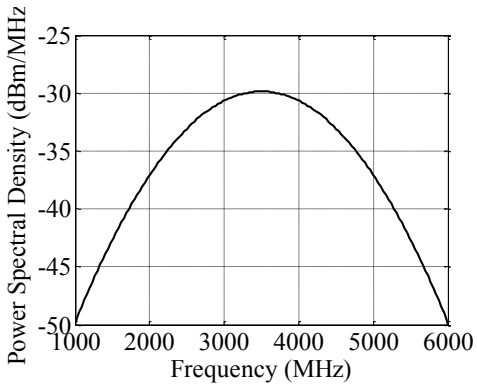

Figure 2. Power spectral density of the excitation pulse.

III. Simulation Results

The path loss represents the average attenuation of a signal as it propagates from a radiation source to a receiving point. The total received energy at each probe in Fig. 1 was obtained by integrating the Poynting vector, $S_{u,v,w}(t)$, during an observation time interval. The Poynting vector can be written as

$$S_{u,v,w}(t) = E_{u,v,w}(t) \times H_{u,v,w}(t) \quad \text{W/m}^2 \qquad (1)$$

where $E_{u,v,w}(t)$ and $H_{u,v,w}(t)$ are the electric and magnetic field, respectively. Because the plane wave was polarized in the *v*-axis direction, the co-polarized field intensity inside the body was significantly larger compared to the cross-polarized field. Thus, only E_y and H_u were calculated, which means that the power flow direction was along the *w*-axis. The UWB signal energy density, which was received inside the body at different depths from the body surface, was calculated by integrating the power density over the whole observation time, i.e., a time interval sufficiently large to include 99% of the signal energy. Hence, the signal energy was computed as

$$e_w = \int_t |S_w(t)|\, dt, \qquad \tau_0 < t < \tau_{\max} \quad \text{J/m}^2 \qquad (2)$$

where τ_0 and τ_{max} delimit the time window of the received signal energy for the selected links inside the thorax.

A. Path Loss without Matching Layer

Although the probes were arranged in several planes that formed a cubic shape as described previously, the contour of the chest surface was not a straight line. Therefore, the path loss at each individual probe was computed and the average path loss was computed when no matching layer was applied on the torso, i.e., when the environment surrounding the torso was the air. A simple power law function was fitted to the average path loss curve, which is depicted in Fig. 3 by the solid blue line for $\varepsilon_r = 1$. The path loss variations around the average value are known as scattering, and its statistical characterization is necessary for the calculation of the link margin. The scattering is caused by the different dielectric properties of the tissues surrounding each probe and it increases with the depth. For simplicity, the probability density function (PDF) of the scattering (in decibels) was approximated by a single function regardless of depth. The scattering was modeled as a Gaussian distributed random variable (RV), $\mathcal{N}$, with zero mean and standard deviation σ, which can be written like $\mathcal{N}(0,\sigma)$. Hence, the average propagation loss in decibels as a function of depth including the scattering term is given by

$$L_{[\mathrm{dB}]}(d) = L_{0[\mathrm{dB}]} + a(d/d_0)^n + \mathcal{N}(0,\sigma) \qquad (3)$$

where d is the depth from the skin in millimeters ($1 < d < 100$), a is a fitting constant, d_0 is the reference depth equal to 1 mm, L_0 is the loss at the reference depth, and n is an empirical path loss exponent. The parameters for $\varepsilon_r = 1$ are given in Table I.

B. Path Loss with Matching Layer

Similarly to the previous case, the corresponding average path loss for the different permittivity values (i.e., matching layers) was computed. In all these cases, the average path loss can be represented by (3) with the parameters summarized in Table I. Figure 3 shows the corresponding average path loss fitted curves versus depth for these different permittivity values. As seen, by increasing the permittivity of the matching layer the path loss reduces progressively up to $\varepsilon_r = 20$. For instance, for 30 mm depth the path loss without a matching layer is 31 dB, whereas this value is reduced to 22 dB for $\varepsilon_r = 20$. For $\varepsilon_r > 20$ the path loss progressively increases. Therefore, the recommended permittivity value for the matching layer should not exceed $\varepsilon_r = 20$.

IV. Selection of the Matching Layer Permittivity

In order to facilitate the selection of the appropriate permittivity value for a matching layer to be used in a biomedical application with a required depth in the thorax, we depicted Fig. 3 so that the effects of permittivity are highlighted. Hence, Fig. 4 shows the path loss versus both depth and permittivity.

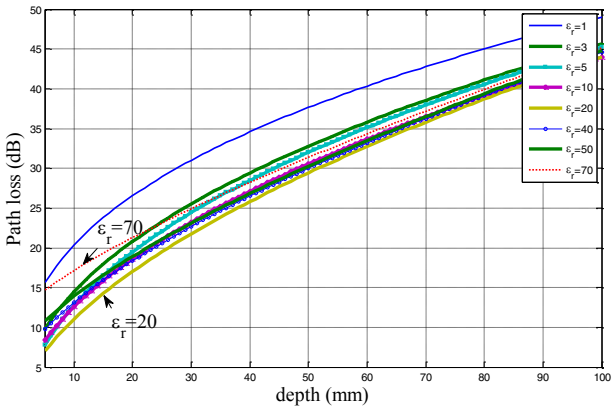

Figure 3. Average path loss versus depth.

TABLE I. Propagation Parameters

ε_r	a	n	$L_{0\,[\mathrm{dB}]}$	$\sigma_{[\mathrm{dB}]}$
1	8.772	0.3754	–0.45	7.23
3	6.339	0.443	–3.08	6.74
5	7.35	0.4251	–6.79	6.63
10	4.58	0.5003	–1.88	5.91
20	3.557	0.5543	–1.68	5.38
30	3.007	0.5834	0.1	5.08
40	2.168	0.6373	3.75	4.89
50	1.843	0.665	5.4	5
60	1.380	0.710	8.3	5
70	1.086	0.7496	11.08	4.92

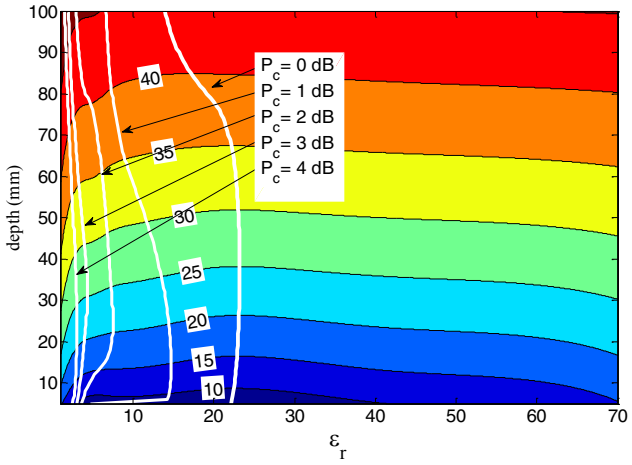

Figure 4. Average path loss versus depth and permittivity.

In order to provide a guideline for the selection of the appropriate permittivity for a target depth, we defined a compression level, P_c. This parameter is the number of acceptable decibels below the maximal path loss reduction for a given depth. Obviously, the maximal path loss reduction value has a compression level of $P_c = 0$ dB. Other values for P_c that we defined were P_c = 1, 2, 3 and 4 dB.

The vertical curves in Fig. 4 correspond to each of the defined P_c values and help to select the adequate permittivity for a given depth. For example, if a biomedical application requires a UWB signal reaching a depth of $d = 90$ mm, then the optimal dielectric material for the matching layer must have a permittivity of $\varepsilon_r = 15$. This value can be obtained by tracing a horizontal line from the value of 90 mm in the vertical axis until it intersects the curve corresponding to $P_c = 0$ dB; then, a vertical line is traced down from this point to the horizontal axis in order to find the permittivity. As the $P_c = 0$ dB curve clearly denotes, the most recommended permittivity value for the optimal matching layer lies within $14 < \varepsilon_r < 22$ depending on the depth.

Figure 4 can be also used to evaluate the quality of a selected material for a matching layer. From a practical point of view, the recommended permittivity obtained with the guideline described above cannot always be matched with existing materials. In such a case, different materials with known permittivity can be considered and their quality as a matching layer can be roughly evaluated in terms of their corresponding P_c value. Smaller values of P_c must be always favored for the physical implementation of a matching layer.

V. Conclusions

We have investigated the effects of a dielectric matching layer on the path loss suffered by an ultra wideband electromagnetic wave propagating into the human thorax in the 1-6 GHz frequency range. Our simulations have evidenced that a matching layer of dielectric material with the properly selected permittivity value can reduce the propagation loss. This path loss reduction can reach a value of up to 10 dB, but in most cases the improvement is smaller and it depends on the depth inside the body. We provided the guidelines for determining the optimal value of permittivity for a matching layer, which lies between $\varepsilon_r = 14$ and $\varepsilon_r = 22$ for the considered depths. However, when the optimal permittivity value cannot be used for practical reasons, the suitability for a matching layer of different materials with known permittivity can be assessed with the results we have provided. This is an important contribution that can greatly help designers of biomedical devices operating with ultra wideband signals.

The concept of a matching layer can have potential application in the design of wireless capsule endoscope communication systems operating with ultra wideband signals. The receiver antenna elements can be embedded in an appropriate dielectric material inside the belt that a patient has to wear during a capsule endoscopic procedure. However, for this sake the simulations have to be done for the abdomen and larger depths (up to 500 mm) shall be considered. Our future work will investigate this application.

References

[1] K. Sayrafian-Pour, W.-B. Yang, J. Hagedorn, J. Terrill, K. Y. Yazdandoost, and K. Hamaguchi, "Channel models for medical implant communication," *Intl. J. of Wireless Information Networks*, vol. 17, no. 3–4, pp. 105–112, Dec. 2010.

[2] R. Chávez-Santiago, K. Sayrafian-Pour, A. Khaleghi, K. Takizawa, J. Wang, I. Balasingham, and H.-B. Li, "Propagation models for IEEE 802.15.6 standardization of implant communication in body area networks," *IEEE Commun. Mag.*, vol. 51, no. 8, pp. 80–87, Aug. 2013.

[3] R. Chávez-Santiago, and I. Balasingham, "The ultra wideband capsule endoscope," in *Proc. IEEE Intl. Conf. on Ultra-Wideband (ICUWB)*, Sydney, Australia, Sep. 15–18, 2013, pp. 72–78.

[4] J. Zhu, "Optimization of matching layer design for medical ultrasonic transducer," Ph.D. dissertation, The Pennsylvania State Univ., PA, 2008.

[5] A. Khaleghi, R. Chávez-Santiago, and I. Balasingham, "On the use of a dielectric matching layer for ultra wideband medical applications," in *Proc. 7th Intl. Conf. on Body Area Networks (BodyNets)*, Oslo, Norway, Sep. 24–26, 2012, pp. 69–75.

[6] Q. Wang, K. Wolf, and D. Plettemeier, "An UWB capsule endoscope antenna design for biomedical communications," in *Proc. 3rd Intl. Symp. on Applied Sciences in Biomedical and Communication Technologies (ISABEL)*, Rome, Italy, Nov. 7–10, 2010, pp. 1–6.

[7] E. Gjonaj, M. Bartsch, M. Clemens, S. Schupp, and T. Weiland, "High-resolution human anatomy models for advanced electromagnetic field computations," *IEEE Trans. Magn.*, vol. 38, no. 2, pp. 357–360, Mar. 2002.

[8] C. Gabriel, "Compilation of the dielectric properties of body tissues at RF and microwave frequencies," Brooks Air Force, N.AL/OE-TR-1996-0037, San Antonio, TX, 1996.

[9] A. Khaleghi, I. Balasingham, and R. Chávez-Santiago, "Computational study of ultra-wideband wave propagation into the human chest," *IET Microwaves, Antennas & Propagation*, vol. 5, no. 5, pp. 559–567, Apr. 2011.